ARCHIVES OF ELECTRICAL ENGINEERING VOL. 67(2), pp. 333–343 (2018)

DOI 10.24425/119644

Experimental verification of Dead-Beat predictive current controller for small power, low speed PMSM

RYSZARD PAŁKA[1], RAFAŁ PIOTUCH[2]

[1] *West Pomeranian University of Szczecin, Poland*
e-mail: ryszard.palka@zut.edu.pl

[2] *ABM Greiffenberger Antriebstechnik GmbH Germany*
e-mail: rafal.piotuch@abm-antriebe.de

(Received: 30.10.2017, revised: 05.02.2018)

Abstract: This paper presents simulation and experimental results obtained with a Dead-Beat predictive current controller for a Permanent Magnet Synchronous Machine (PMSM) drive system. With means of combined field and circuit simulations, an efficiency map and required current in a direct- and quadrature-axis are defined. A control algorithm was implemented within an open-interface inverter from Texas Instruments. Dynamic response for both axis currents was defined and verified as well as current ripples for different set currents in the quadrature axis.

Key words: current controller, PM motors, dead-beat, FEM, efficiency map

1. Introduction

Over the last 4 decades a big improvement has been made in the analysis and design process of electrical machines, mainly due to improved computer capabilities and advancements in material engineering. Probably all new electrical machines are designed, analyzed and optimized with a help of field simulations that concern details of geometry, material characteristics and different power supply conditions including faulty states [1–8]. This allows to approximate such parameters and characteristics as inductances, core losses, field weakening capabilities and efficiency maps or predict behavior of a drive in faulty conditions with sufficient accuracy for a big range of applications. Not without significance is development done in the field of control algorithms, sensorless control systems and Digital Signal Processors dedicated to electrical drives which as well use more and more often combined Finite Element and circuit simulations.

Predictive algorithms are based on a simplified mathematical description of phenomena occurring in electrical machines. Over the last 2 decades there is a big interest in predictive control

algorithms. The first industrial system with a predictive off-line method was implemented by ABB in the 80's of the XX century. It's called the Direct Torque Control (DTC) method and beside the Field Oriented Control (FOC) method it is one of the commonly used control schemes. To develop a predictive algorithm there is a need to define main electromagnetic parameters of a controlled motor. These parameters are regularly obtained with the FEM. In practical implementations of predictive controllers constrains and time delays should be defined and considered.

2. Test Bench and main motor parameters

The tested object was a self-designed 6-pole IPM synchronous motor with NdFeB magnets of $B_r = 1.21$ T. Main electromagnetic parameters that required the development of the Dead-Beat current controller are presented in Table 1. The parameters were defined for 60°C. The test bench consisting of a Tektronix scope, IPM, an inverter from Texas Instruments and DC power supply is presented in Fig. 1.

Table 1. Main motor parameters

Parameter	Value	Unit	Description
p	3	–	number of pole pairs
L_d	16	mH	d-axis inductance
L_q	25	mH	q-axis inductance
ψ_{pm}	0.138	Vs	PM flux amplitude
R	4.7	ohm	phase resistance
T	3.21	Nm	torque
d_o	90	mm	outer stator diameter
L_{st}	40	mm	stack length
I_n	3.5	A	nominal phase current
U_{dc}	120	V	DC bus voltage

Nominal speed of a motor was strongly limited because of limitation caused by power supply (voltage) as well as inverter power switches and sensing circuits (current).

The inverter is an opened interface inverter from Texas Instruments equipped with F283335 Delfino CPU. Sampling time (T_s) of the inverter is set to 100 μs, DC bus voltage is set to 80 V (because of power supply limit). The Space Vector Modulation method has been used. Measurements were done with internal inverter circuits – shunt resistors and with the Rogowski coil.

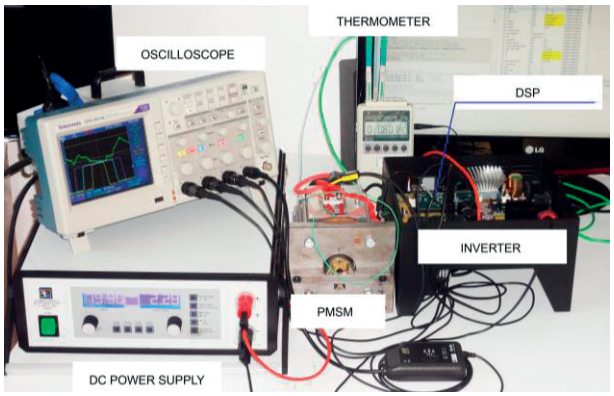

Fig. 1. Test bench view

3. Motor parameters and characteristics

Several parameters like no-load voltage, or self- and mutual inductances need to be defined. These parameters are very important in electromagnetic analysis and design as well as for a control algorithm design process. They could be used as an indicator in the first phase of the design, but in each case a detailed analysis is necessary [3–7].

Some exemplary construction details of one of analyzed machines and the field plot are shown in Fig. 2a and Fig. 2b, respectively. The no-load voltage waveform as well as its harmonics obtained from the experimental test and FEM calculations for final geometry are presented in Fig. 3a and Fig. 3b, respectively.

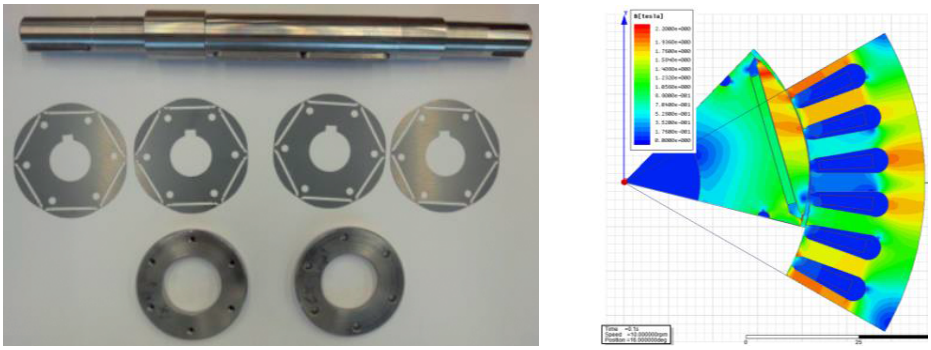

(a) (b)

Fig. 2. (a) Construction details of one of designed machines; (b) exemplary magnetic field distribution

The first harmonic in the measured voltage is very high compared to all other harmonics. During the measurement a third harmonic component can be seen, but this could be caused by a measurement error. Correspondence between the FEM and the experimental results is on a very high level.

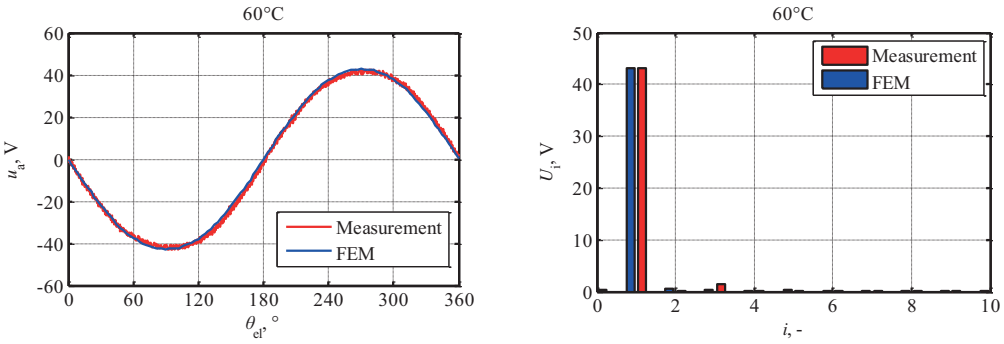

(a) (b)

Fig. 3. (a) No-load phase voltage waveform; (b) no-load phase voltage waveform harmonic components

3.1. Motor maps

Inductances are crucial parameters of an electrical machine. They define machine capability in the field weakening region, current ripples, power factor and required inverter parameters. Based on the waveforms of self- and mutual inductances it is possible to estimate d and q inductance values – some procedures have been presented in [3]. The ratio of q-axis to d-axis inductance for the analyzed motor equals 1.6 for nominal supply conditions.

Based on data obtained mainly with FEM calculation and shown in Table 1, different types of maps may be defined. Exemplary maps are presented in Figs. 4–6. The maps were generated for 120 V DC bus voltage.

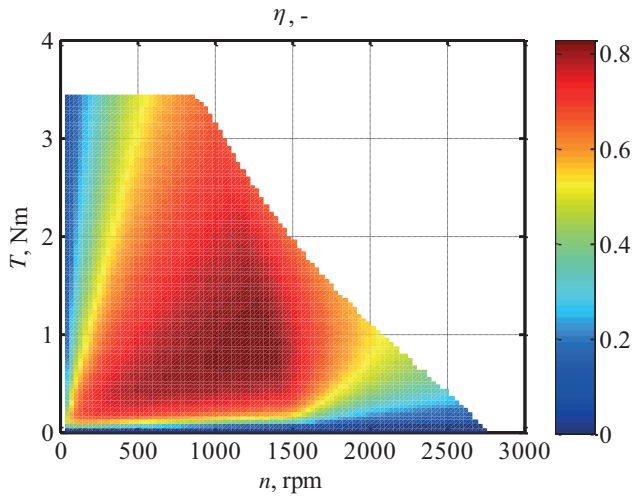

Fig. 4. Efficiency map

All the obtained maps and parameters may be used either in motor or control system design procedure.

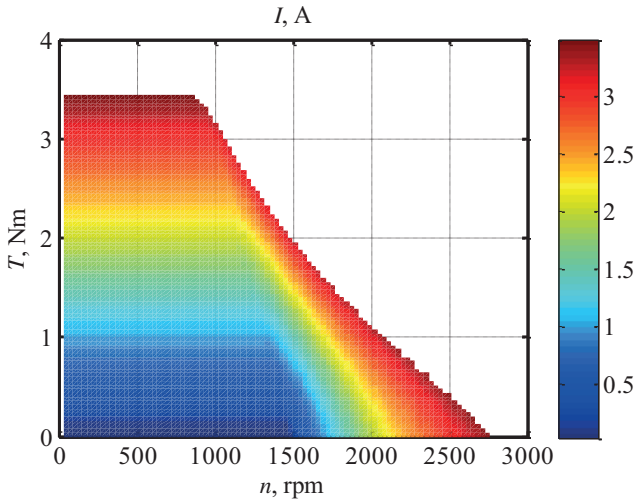

Fig. 5. Current map

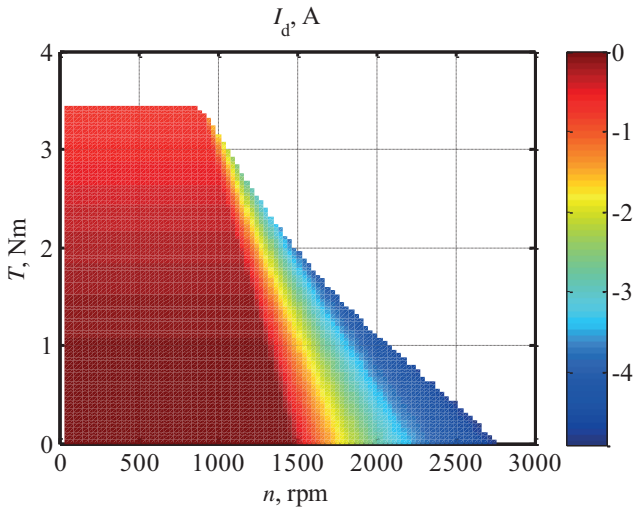

Fig. 6. *d*-axis current map

4. Dead-beat predictive controller

Each control system, which uses information of an object in order to develop optimal control signals can be included to predictive controllers group [5, 10]. Fig. 7. presents a predictive current controller scheme. A cost function block is able to select the best current vector in a next sampling time. Accuracy of prediction is dependent on accuracy of a motor model.

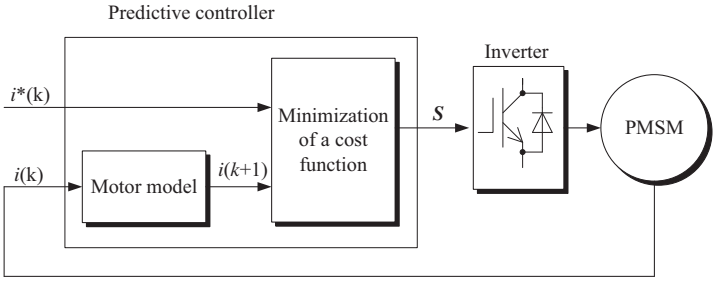

Fig. 7. Basic scheme for a predictive current controller

A cost function that has to be minimized may be defined, in a very simple but effective way, as an angle or distance between set current and predicted current value. A Dead-beat controller does not minimize a cost function in a direct manner but uses the mathematical description of an object and inverter to directly move predicted current values in the next sampling step (in fact in two steps) as near as possible to the set current value.

The idea of minimization of a cost function is presented in Fig. 8. The best power switch configuration (according to selected cost function) is configuration number 3 – S_3. All the other power switch configurations that could be applied lead to the worst control quality.

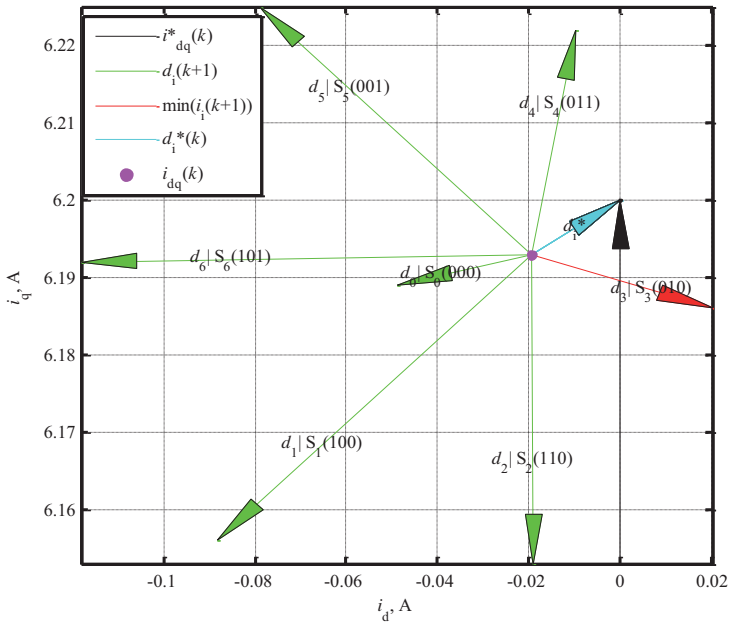

Fig. 8. Predicted directions of change of current vector for 8 key configurations (d_x – predicted current change for x key configuration, x – number of key configuration, S_x – upper switches configuration with states of subsequent power switches)

Electromagnetic torque neglecting cogging torque may be described as follows:

$$T = \frac{3}{2} \cdot p \cdot [\psi_{pm} \cdot i_q + (L_d - L_q) \cdot i_d \cdot i_q], \tag{1}$$

where: i_d and i_q are the d- and q-axis current components. The first term in Equation (1) is the PM generated torque, and the second term is the reluctance torque which is proportional to the difference in inductances L_d and L_q. In the analyzed IPMSM, L_q is higher than L_d. A basic mathematical model for IPM machines is presented by the following equation set:

$$u_d = R \cdot i_d + \frac{\mathrm{d}\psi_d}{\mathrm{d}t} - p \cdot \omega_m \cdot \psi_q, \tag{2}$$

$$u_q = R \cdot i_q + \frac{\mathrm{d}\psi_q}{\mathrm{d}t} - p \cdot \omega_m \cdot \psi_d, \tag{3}$$

$$\psi_d = L_d i_d + \psi_{pm}, \tag{4}$$

$$\psi_q = L_q i_q, \tag{5}$$

where: ψ_d and ψ_q represent the flux in the d- and q-axis respectively; u_d and u_q are the d- and q-axis voltage components.

Based on the presented model, following matrices have been defined:

$$\boldsymbol{A}(k) = \begin{bmatrix} 1 - \dfrac{R \cdot T_s}{L_d} & T_s \cdot \dfrac{L_q}{L_d} \cdot \omega(k) \\ -T_s \cdot \dfrac{L_d}{L_q} \cdot \omega(k) & 1 - \dfrac{R \cdot T_s}{L_q} \end{bmatrix}, \tag{6}$$

$$\boldsymbol{B} = \begin{bmatrix} \dfrac{T_s}{L_d} & 0 \\ 0 & \dfrac{T_s}{L_q} \end{bmatrix}, \qquad \boldsymbol{C}(k) = \begin{bmatrix} 0 \\ -\dfrac{T_s \cdot \omega(k)}{L_q} \cdot \psi_{pm} \end{bmatrix}, \tag{7}$$

$$\boldsymbol{i}_{dq}(k) = \begin{bmatrix} i_d(k) \\ i_q(k) \end{bmatrix}, \qquad \boldsymbol{u}_{dq}(k) = \begin{bmatrix} u_d(k) \\ u_q(k) \end{bmatrix}. \tag{8}$$

Considering Equations (1–8) it is possible to define the required voltage vector signal to reach set current values:

$$\boldsymbol{u}_{dq}(k+1) = \boldsymbol{B}^{-1}(\boldsymbol{i}^*_{dq}(k) - \boldsymbol{A}(k) \cdot \boldsymbol{i}_{dq}(k+1) - \boldsymbol{C}(k), \tag{9}$$

where $\boldsymbol{i}_{dq}(k+)$ is the estimated or predicted current value at the end of an actual sampling period. The Dead-Beat predictive current controller scheme is presented in Fig. 9.

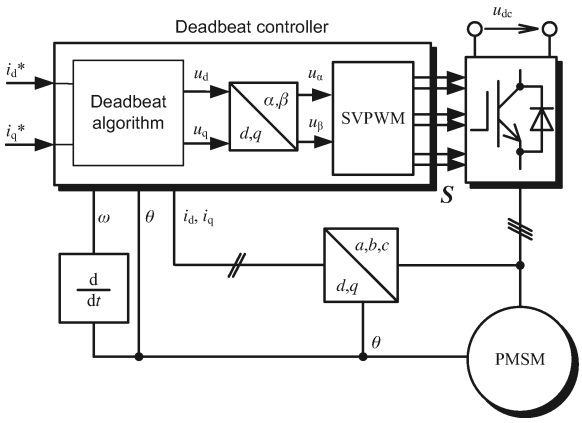

Fig. 9. Dead-beat current controller scheme

5. Test results

Among several required features of a control algorithm there are some critical ones [10–16]. Of main importance is the system stability. The controller needs to assure stable behavior for different speeds, torques and conditions. This may be evaluated using control theory and mathematical description [9, 12, 15], but because of system complexity and non-linearity it is normally defined by simulation and test. The second important issue is rising time of a current which assures proper dynamic behavior of a drive. The last crucial issue is a current ripple. It is defined as a pk2pk value of currents in both axes for defined speed and other drive conditions. Because of several issues it is recommended to test current ripples with a blocked shaft. This is only one working point and rather rare, but it allows to define current controller performance very precisely and separate all additional issues related to speed loop control quality, natural torque ripples, etc.

Stability of the system was tested for many hours and hundreds of start-stop procedures. The whole system worked well without excessive noise. Samples of experimental and simulation data are presented in Fig. 10–12. Rise time for a q-current axis is around 7 ms for the analyzed system.

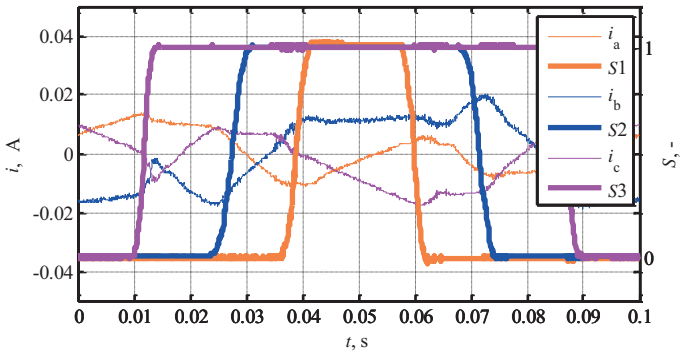

Fig. 10. Gate signals and corresponding phase current waveforms

Difference between simulation and experimental results is negligible. It proves that a proper FEM simulation allows to obtain a model of very high accuracy (at least for regular motors without extreme nonlinearities).

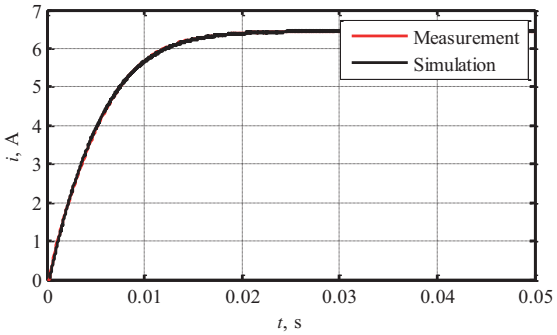

Fig. 11. Dynamic q-axis current response

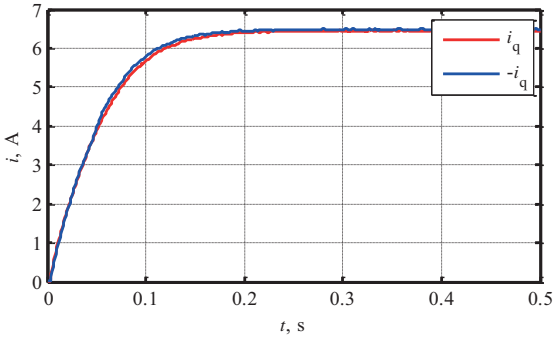

Fig. 12. Dynamic q-axis current response experimental results

In Table 2 there are defined pk2pk current error values for the d- and q-axis. A current ripple in the q-axis is nearly always higher than a current ripple in the d-axis. It is caused by different

Table 2. Pk2pk current values comparison

	pk2pk(e(i_d))		pk2pk(e(i_q))	
I_q, A	**Experiment**	**Simulation**	**Experiment**	**Simulation**
1	0.0161	0.0126	0.0159	0.0141
2	0.0272	0.0215	0.0314	0.0234
3	0.0369	0.0301	0.0307	0.0263
4	0.0528	0.0445	0.0410	0.0375
5	0.0639	0.0573	0.0419	0.0414
6	0.0754	0.0695	0.0420	0.043

inductances. The relative current ripple in the q-axis is around 1.2% for nominal current, which is a small value for a great number of applications. The current ripple rises with a set current value ranging from 0.012–0.070 A for the simulation and 0.016–0.075 A for the experiment. The correspondence of the obtained results stays on a high level.

6. Summary and conclusions

The Dead-Beat predictive current controller performed well during tests. The system worked without any problems for different set current values. It presented excellent dynamic response for currents in both axes. Motor parameters that have been obtained from the FEM have made it possible to achieve proper drive performance. The simulation results of the whole system have been validated against the experimental data showing high accuracy of the simulation results. The tests were limited to a small temperature range only and only one motor and inverter sample in laboratory conditions, but they proved that the Dead-Beat controller could be an excellent (regarding performance) and reasonable solution (regarding implementation costs and complexity) for current control in FOC control systems for small power PMSMs.

Acknowledgements

This work has been supported with the grants of the National Science Centre, Poland 2014/15/N/ST8/03396 and 2015/17/B/ST8/03251.

References

[1] Zarko D., Ban D., Klari R., *Finite Element Approach to Calculation of Parameters of an Interior Permanent Magnet Motor*, AUTOMATIKA, vol. 46, no. 3–4, pp. 113–122 (2006).

[2] Młot A., Łukaniszyn M., Korkosz M., *Magnet loss analysis for a high-speed PM machine with segmented PM and modified tooth-tips shape*, Archives of Electrical Engineering, vol. 65, no. 4, pp. 671–683 (2016).

[3] Stumberger B. *et al*., *Evaluation of Saturation and Cross-Magnetization Effects in Interior Permanent-Magnet Synchronous Motor*, IEEE Transactions on Magnetics, vol. 39, no. 5, pp. 1264–1271 (2003).

[4] Di Barba P., Mognaschi M.E., Bonisławski M., Pałka R., Paplicki P., Piotuch R., Wardach M., *Hybrid Excited Synchronous Machine with Flux Control Possibility*, International Journal of Applied Electromagnetics and Mechanics, vol. 52, no. 3–4, pp. 1615–1622 (2016).

[5] Morel F., Xuefang L.-S., Retif J.-M., Allard B., Buttay C., *A Comparative Study of Predictive Current Control Schemes for a Permanent-Magnet Synchronous Machine Drive*, IEEE Transactions on Industrial Electronics, vol. 56, no. 7 (2009).

[6] Pałka R., *Synthesis of magnetic fields by optimization of the shape of areas and source distributions*, Electrical Engineering 75, pp. 1–7 (1991).

[7] Caramia R., Piotuch P., Pałka R., *Multiobjective FEM based optimization of BLDC motor using Matlab and Maxwell scripting capabilities*, Archives of Electrical Engineering, vol. 63, no. 1, pp. 115–124 (2014).

[8] Bonisławski M., Pałka R., Paplicki P., Wardach M., *Unconventional control system of hybrid excited synchronous machine*, 20th International Conference on Methods and Models in Au-

tomation and Robotics (MMAR 2015), IEEE Conference Publications, pp. 649–654 (2015), DOI: 10.1109/MMAR.2015.7283951.

[9] Paplicki P., Wardach M., Bonisławski M., Pałka R., *Simulation and experimental results of hybrid electric machine with a novel flux control strategy*, Archives of Electrical Engineering, vol. 64, pp. 37–51 (2015), DOI: 10.1515/aee-2015-0005.

[10] Cortés P., Kaźmierkowski M.P., Kennel R.M., Quevedo D.E., Rodríguez J., *Predictive Control in Power Electronics and Drives*, IEEE Transactions on Industrial Electronics, vol. 55, no. 12 (2008).

[11] Jarzębowicz L., Opaliński A., Cisek M., *Improving control dynamics of PMSM drive by estimating zero-delay current value*, Elektronika ir Elektrotechnika, vol. 21, no. 2 (2015).

[12] Nalepa R., Orłowska-Kowalska T., *Optimum Trajectory Control of the Current Vector of a Nonsalient-Pole PMSM in the Field-Weakening Region*, IEEE Transactions on Industrial Electronics, vol. 59, no. 7 (2012).

[13] Piotuch R., Pałka R., *Adaptive Deadbeat Current Controller for IPMSM*, 21st International Conference on Methods and Models in Automation and Robotics (MMAR 2016), IEEE Conference Publications, pp. 300–305 (2016), DOI: 10.1109/MMAR.2016.7575151.

[14] Piotuch R., Pałka R., *Dead-Beat predictive current controller for PMSM*, International Symposium on Electrical Machines (SME) 2017, DOI: 10.1109/ISEM.2017.7993574.

[15] Jarzębowicz L. Opaliński A., *Frequency and time domain characteristics of digital control of electric vehicle in-wheel drives*, Archives of Electrical Engineering, vol. 66, no. 4, pp. 829–842 (2017).

[16] Vu N.T.-T., Choi H.H., Kim R.-Y., Jung J.-W., *Robust speed control method for permanent magnet synchronous motor*, IET Electr. Power Appl., vol. 6, iss. 7, pp. 399–411 (2012).